Eur J Nucl Med Mol Imaging (2015) 42:2029–2037
DOI 10.1007/s00259-015-3119-1

ORIGINAL ARTICLE

A pilot study imaging integrin αvβ3 with RGD PET/CT in suspected lung cancer patients

Song Gao[1,2] · Honghu Wu[3] · Wenwu Li[4] · Shuqiang Zhao[4] · Xuepeng Teng[4] · Hong Lu[4] · Xudong Hu[1] · Suzhen Wang[1] · Jinming Yu[1] · Shuanghu Yuan[1]

Received: 16 March 2015 / Accepted: 14 June 2015 / Published online: 9 July 2015

Abstract
Purpose Angiogenesis is an essential step in tumour development and metastasis. Integrin αvβ3 plays a major role in angiogenesis, tumour growth and progression. A new tracer, ^{18}F-AL-NOTA-PRGD2, denoted as ^{18}F-alfatide, has been developed for positron emission tomography (PET) imaging of integrin αvβ3. This is a pilot study to test the safety and diagnostic value of ^{18}F- arginine-glycine-aspartic acid (RGD) PET/computed tomography (CT) in suspected lung cancer patients.
Methods Twenty-six patients with suspected lung cancer on enhanced CT underwent ^{18}F-alfatide RGD PET/CT examination before surgery and puncture biopsy. Standard uptake values (SUVs) and the tumour-to-blood ratios were measured, and diagnoses were pathologically confirmed.
Results RGD PET/CT with ^{18}F-alfatide was performed successfully in all patients and no clinically significant adverse events were observed. The ^{18}F-alfatide RGD PET/CT analysis correctly recognized 17 patients with lung cancer, 4 patients (hamartoma) as true negative, and 5 patients (4 chronic inflammation and 1 inflammatory pseudotumour) as false positive. The sensitivity, specificity, accuracy, positive predictive value (PPV) and negative predictive value (NPV) of ^{18}F-alfatide RGD PET/CT for the diagnosis of suspected lung cancer patients was 100, 44.44, 80.77, 77.27, and 100 %, respectively. The area under a receiver operating characteristic (ROC) curve was 0.75 (P=0.038), and ROC analysis suggested an SUVmax cut-off value of 2.65 to differentiate between malignant lesions and benign lesions. The SUV for malignant lesions was 5.37±2.17, significantly higher than that for hamartomas (1.60±0.11; P<0.001). The difference between the tumour-to-blood ratio for malignant lesions (4.13±0.91) and tissue of interest-to-blood ratio for hamartomas (1.56±0.24) was also statistically significant (P<0.001). Neither the SUVmax nor the tumour-to-blood ratio was significantly different between malignant lesions and inflammatory lesions or inflammatory pseudotumours (P>0.05). Sixteen of 26 patients later underwent successful surgery, and pathologic examination confirmed nodes positive for metastasis in 14 of 152 lymph nodes. The sensitivity, specificity, accuracy, PPV, and NPV of PET/CT for lymph nodes was 92.86, 95.65, 95.40, 61.90, and 99.25 %, respectively.
Conclusion Our results suggest that RGD PET/CT with the new tracer ^{18}F-alfatide is safe and potentially effective in the diagnosis of non-small cell lung cancer. It may be used in the diagnosis of lung cancer, successfully distinguishing malignant lesions from hamartoma. However, it is difficult to clearly differentiate inflammatory or inflammatory pseudotumours from malignant lesions. Additional studies with a larger number of patients are needed to validate our findings.

Keywords Integrin $\alpha v\beta_3$ · Lung cancer · RGD PET · ^{18}F-alfatide

✉ Shuanghu Yuan
yuanshuanghu@sina.com

[1] Department of Radiation Oncology, Shandong Cancer Hospital & Institute, No 440 Jiyan Road, Jinan, Shandong 250117, China

[2] School of Medicine and Life Sciences, University of Jinan-Shandong Academy of Medical Sciences, Jinan, Shandong, China

[3] Wuyi County People's Hospital of Hengshui City, Hengshui, Hebei Province, China

[4] Department of Radiology, Shandong Cancer Hospital & Institute, Jinan, Shandong, China

Introduction

Angiogenesis, the growth of new blood vessels from pre-existing vessels, is a key process in tumour growth and metastasis. Tumour angiogenesis could potentially be utilized for the diagnosis of malignancies and for cancer therapeutics. In 1971, Folkman first articulated the importance of angiogenesis for tumour growth, without which a tumour cannot grow larger than a few millimetres in diameter [1]. In the following years, angiogenesis and anti-angiogenic therapy became one of the most important fields of oncological research. Anti-angiogenic therapies are designed to normalize abnormal blood vessels found in tumours and their hemodynamic parameters (e.g., blood flow and vascular permeability) [2]. Today, there are numerous anti-angiogenesis targeted drugs in clinical use; for example, bevacizumab (Avastin), vandetanib (ZD6474), sunitinib, sorafenib, and endostar [3].

Integrins are heterodimeric transmembrane glycoproteins, which play an important role in cell–cell and cell–matrix interactions. They have been widely studied and play key roles in angiogenesis and tumour metastasis [4]. The integrin family is a group of transmembrane glycoproteins comprised of 18α- and 8β- subunits that are expressed in 24 different α/β heterodimeric combinations on the cell surface. Among the 24 members of the integrin family, integrin αvβ3 is studied the most extensively for its role in tumour growth, progression, and angiogenesis. Integrin αvβ3 is significantly up-regulated in various types of tumour cells and the activated endothelial cells of tumour angiogenesis but not at all or very little in quiescent vessel cells and other normal cells [4–6]. Therefore, imaging αvβ3 expression can help to evaluate tumour neovascularization, and the integrin αvβ3 receptor is a valuable target for the diagnosis and treatment of malignant tumours [7, 8].

Because the tripeptide sequence of arginine-glycine-aspartic acid (RGD) can specifically bind to the integrin αvβ3 receptor [9, 10], various RGD-containing peptide probes have been tested. Because PET imaging has the advantage of being very sensitive to low concentrations of tracer molecules that can detect picomolar radiotracer concentrations and because it has unlimited depth penetration, PET radiotracer targeting αvβ3 expression is the most intensively studied strategy for imaging tumour angiogenesis [11]. RGD peptides have been radiolabeled and evaluated with radionuclides including ^{18}F [12], ^{68}Ga [13, 14], ^{64}Cu [15], ^{76}Br [16], and ^{89}Zr [17], which have successfully been used clinically in integrin αvβ3–targeted PET imaging.

Of the RGD radiotracers, ^{18}F is the most popular radioisotope for labelling peptides, because its half-life (109.7 min) is well suited for routine clinical use. Various ^{18}F-labelled RGD peptide tracers have been tested, including ^{18}F-galacto-RGD [18–21], ^{18}F-AH111585 [22, 23], ^{18}F-RGD-K5 [24], ^{18}F-FPRGD2 and ^{18}F-FPPRGD2 [25] These were approved for study under an exploratory investigative new drug application with the USA Food and Drug Administration (FDA). All of them are safe to use, and have desirable pharmacokinetic and biodistribution properties. They can be used in PET evaluation of oncologic patients for several types of tumours, including breast cancer [23, 26], malignant glioma [27], and squamous cell carcinoma of the head and neck [28]. These studies have shown that the uptake of all tumours correlated well with the expression of integrin αvβ3. However, the radiochemical syntheses of the ^{18}F-labelled RGD tracers are complex, and automation of these processes is difficult, which limits their widespread use in clinical settings. To improve the synthesis methods, several studies were conducted, which demonstrated that labelling with ^{18}F in a more facile and convenient procedure is feasible. McBride et al. [29] developed and optimized the AlF-labelling technology. They found that the rapid and simple ^{18}F-AlF-labelling method can be easily adapted for preparing heat-sensitive compounds with ^{18}F quickly and in high yields. Based on these studies, ^{18}F-AlF-NOTARGD2 and ^{18}F-AlF-NOTA-PRGD2 were successfully made in a single-step radiosynthesis [30], and showed excellent capability in studies of in vitro serum stability and in vivo tumour imaging. In 2013, Wan et al. [31] developed a simple lyophilized kit for labelling PRGD2 peptide (^{18}F-AlFNOTA-PRGD2, denoted as ^{18}F-alfatide), and conducted the first clinical research using ^{18}F-alfatide RGD PET/CT scans in lung cancer patients. They reported that ^{18}F-alfatide can be produced with excellent radiochemical yield and purity via a simple, one-step lyophilized kit. PET scanning with ^{18}F-alfatide allows specific imaging of αvβ3 expression with good contrast in lung cancer patients.

In this clinical study, we use ^{18}F-alfatide as a new tracer for PET imaging of integrin αvβ3 in lung cancer patients. The objective of the present study was to test the safety of the method, and it is the first investigation of whether ^{18}F-alfatide RGD PET/CT can be used in the diagnostic imaging of lung cancer.

Materials and methods

Patients

This study was approved by the ethics committee of Shandong Cancer Hospital, and each patient gave written and informed consent before the study. All patients were treated in Shandong Cancer Hospital and satisfied the following criteria: (1) suspected lung cancer on enhanced CT; (2) no prior therapy; (3) Karnofsky performance status (KPS) ≥70; (4) ready to undergo surgery or lung puncture biopsy; and (5) age >18 years.

PET scanning

The simple lyophilized kit for labelling PRGD2 peptide was purchased from the Jiangsu Institute of Nuclear Medicine, and the synthesis process was carried out in accordance with previous studies [31]. The radiochemical purity of the ^{18}F-alfatide exceeded 95 %, and its specific radioactivity exceeded 37 GBq (1000 mCi)/μmol. There were no specific subject preparations, patients did not need fasting and did not receive CT contrast agents. ^{18}F-alfatide (213.34±29.8 MBq) was injected intravenously in all patients, who then rested for approximately 60 minutes. Scanning was performed with an integrated in-line PET/CT system (Discovery LS; GE Healthcare). PET emission images were taken from the head to the thigh. The spiral CT component was performed with an x-ray tube voltage peak of 140 kV and 80 mA, a 6:1 pitch, a slice thickness of 4.25 mm, and a rotation speed of 0.8 s per rotation. A full-ring dedicated PET scan of the same axial range followed. The patients were in normal shallow respiration during image acquisition. The images were attenuation corrected with the transmission data from CT. The attenuation-corrected PET images, CT images, and fused PET/CT images displayed as coronal, sagittal, and transaxial slices were viewed on a Xeleris workstation (GE Healthcare).

Image analysis

Two experienced nuclear medicine physicians read all of the images through consensus reading. They were blinded to the clinical and structural imaging findings. PET data were reconstructed using the ordered-subsets expectation maximization algorithm. The SUV was calculated according to the following formula: [measured activity concentration (Bq/mL)×body weight (g)] / injected activity (Bq). In the static emission scans, circular regions of interest (ROIs) with a diameter of 1.5 cm were placed over the arch of the aorta (for measurement of blood activity), heart, lung, liver, thyroid gland, spleen, kidneys, intestine, bone, bladder, muscle, brain and brain ventricles with the assistance of corresponding CT images. The results were expressed in mean SUV. In the tumours, the areas with the maximum intensity were chosen for measurements. Finally, the tumour-to-blood ratios were calculated by SUVtumor/SUVblood.

When an area of a presumed lymph node showed definite uptake that was focally prominent compared with the surrounding tissues and that was not related to normal physiologic uptake, it was considered to be positive for malignancy. A site of increased ^{18}F-alfatide RGD uptake was defined as negative when it was related to the physiologic biodistribution of ^{18}F-alfatide RGD. The areas of maximum intensity were chosen for measurements.

Table 2 SUVs normalized to weight for various organs

Organ	1 h after administration of ^{18}F-alfatide
Primary tumor	5.37±2.17
Metastasis lymph node	2.23±0.43
Metastatic lesions in the bone	4.71±0.96
Brain	0.07±0.02
Muscle	0.43±0.11
Lung	0.55±0.24
Bone	0.71±0.24
Heart	0.92±0.23
Brain ventricles	1.28±0.38
Thyroid gland	2.50±0.66
Liver	3.08±0.90
Intestine	3.80±0.94
Spleen	5.25±1.62
Kidneys	5.86±1.67
Bladder	25.95±8.21

Collection of tissue samples and pathological analysis

All the patients underwent surgery or lung puncture biopsy. The sensitivity and specificity of the ^{18}F-alfatide RGD PET/CT scans were calculated, using tissue diagnosis as the gold standard. During surgery, experienced thoracic surgeons dissected all visible and palpable lymph nodes in the surgical field that were accessible in the hilum and mediastinum, taking into consideration all results from the preoperative imaging examinations, including the results of CT and PET/CT,

Table 1 Demographic profile and the final histological diagnosis of 26 patients with suspected lung cancer

Final histopathology	Patients (n)	Age, years (mean±SD)	Sex ratio (M:F)
Adenocarcinoma	9	63.78±7.55	5:4
Squamous carcinoma	6	61.33±9.95	4:2
Adenosquamous carcinoma	2	68.00±2.83	0:2
Hamartoma	4	58.50±6.86	2:2
Chronic inflammation	4	57.25±9.18	3:1
Inflammatory pseudotumor	1	61	1:0
Total	26	61.62±7.98	15:11

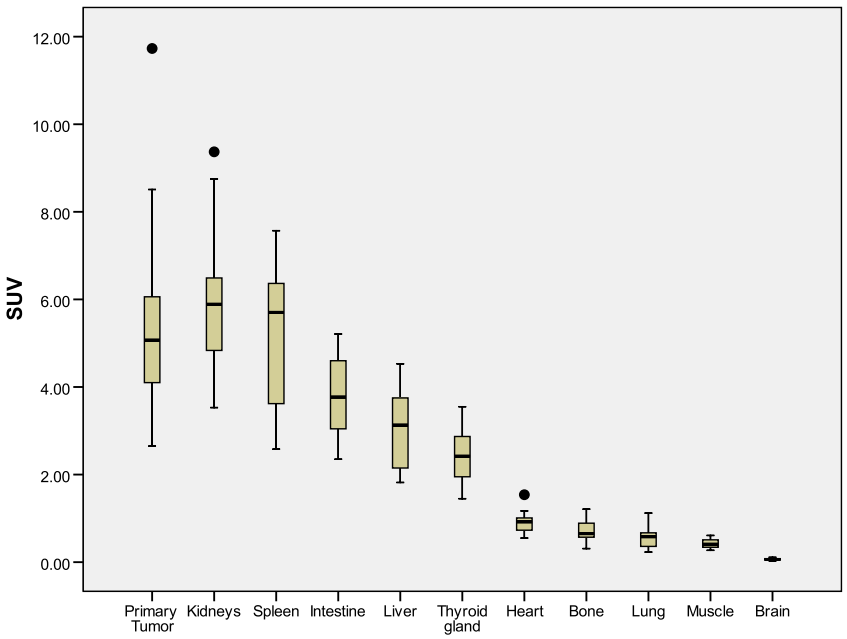

Fig. 1 Box plot diagram of mean SUVs of tumors and normal tissue from static emission scans. Tumor uptake was very heterogeneous but higher than uptake in background tissue, resulting in good image contrast

irrespective of the size of the node [32]. The tumour specimens were immediately fixed in 10-% (volume/volume) formalin, and then embedded in paraffin. Serial 4-μm sections were prepared from each sample for routine hematoxylin and eosin (H&E) staining and immunohistochemical staining. Two pathologists who were unaware of the results used light microscopy to independently assess the slides and arrived at a single final decision between them.

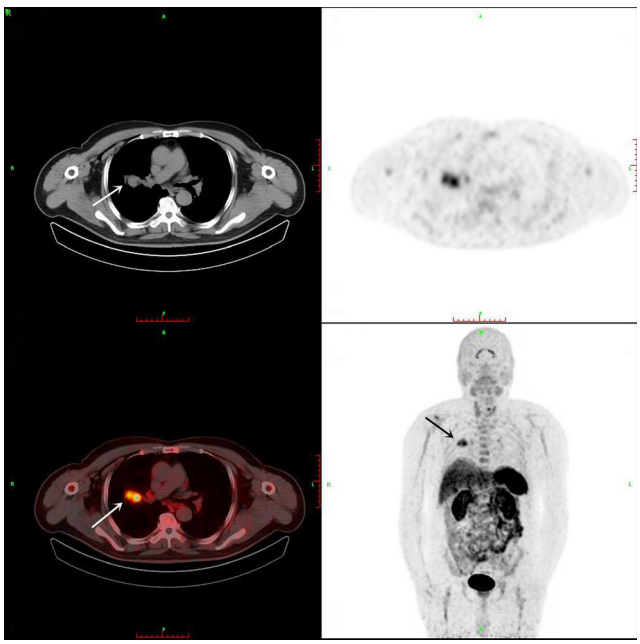

Fig. 2 Major organs and regions of uptake at 1 h after injection of ^{18}F-alfatide in one lung cancer patient. Arrows point to tumor

Statistical analysis

All quantitative data are expressed as the mean±standard deviation (SD). The correlations between tumour size and tumour SUV were assessed using linear regression analysis. Differences between continuous variables and dichotomous variables were tested by one-way ANOVA. The SUV and the tumour-to-blood ratio were compared for benign and malignant lesions and were assessed by the Mann–Whitney U test. Receiver operating characteristic (ROC) curves were generated together with the control dataset, areas under the curve and pertinent 95 % confidence intervals (CIs) were computed, and cut-off points were calculated using the ROC. All statistical tests were carried out using SPSS, version 19.0. Statistical significance was assumed for P values less than 0.05. All P values were two-tailed.

Results

Patient characteristics and safety

The cohort of this study consisted of 26 consecutive patients who met the criteria for inclusion, with a mean age of 61.62± 7.98 years (range, 48–77 years). The patient characteristics are summarized in Table 1. There were 17 patients with malignant lesions and 9 patients with benign lesions. The malignant lesions included adenocarcinoma (n=6), squamous cell carcinoma (n=9), and adenosquamous carcinoma (n=2). The benign lesions consisted of four hamartomas, four cases of chronic inflammation and one inflammatory pseudotumor.

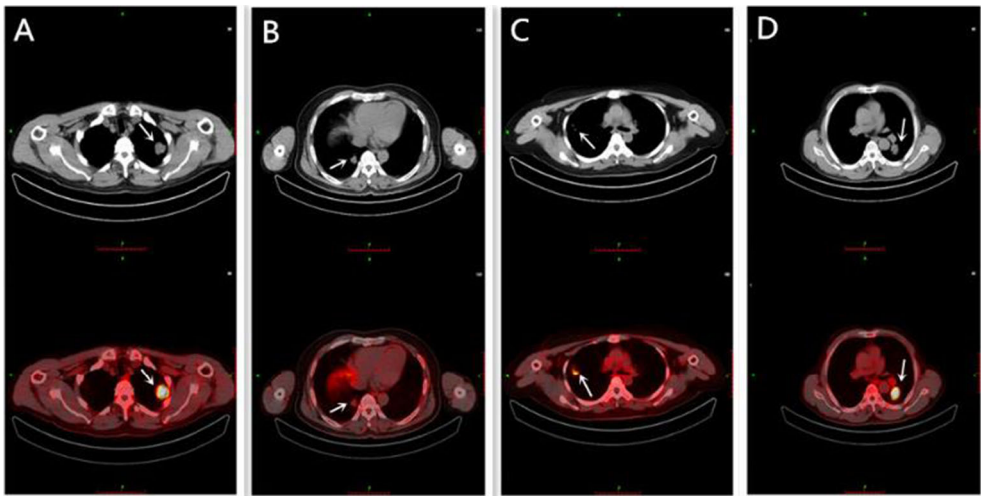

Fig. 3 **a** One patient with lung adenocarcinoma, 1 h after injection of ^{18}F-alfatide, showed high RGD uptake. **b** One patient with hamartoma, 1 h after injection of ^{18}F-alfatide, showed poor RGD uptake. **c** One patient with chronic inflammatory, 1 h after injection of ^{18}F-alfatide, showed definite RGD uptake. **d** One patient with inflammatory pseudotumor, 1 h after injection of ^{18}F-alfatide, showed definite RGD uptake

All of the patients underwent ^{18}F-alfatide RGD PET/CT. After the examination, there were no adverse or clinically detectable pharmacologic effects in any of the subjects. No significant changes in vital signs or the results of laboratory studies or electrocardiograms were observed.

Static emission ^{18}F-alfatide RGD PET scans

All tumours could be identified by ^{18}F-alfatide RGD PET. The results of the SUV measurements for tumours and other major organs are in Table 2 and Fig. 1. The mean SUVs were 5.37±2.17 for tumours, 0.76±0.20 for blood, and 0.43±0.11 for muscle at 1 h after injection. The highest accumulation activity was found in the kidneys and bladder, demonstrating renal clearance. The liver, spleen, and intestines also showed moderate uptake. Minimal radiotracer accumulation was found in the brain, muscle and lung (Fig. 2).

Evaluation of tumours by ^{18}F-alfatide RGD PET/CT scans

All malignant lesions had increased RGD uptake values, with SUVmax values of 5.37±2.17 and tumour-to-blood ratios of 4.13±0.91 (Fig. 3a). Of the nine benign lesions, four patients with hamartoma had a low SUVmax (1.60±1.11) and tissue of interest-to-blood ratios (1.56±0.24) (Fig. 3b). Four patients with chronic inflammation showed definite SUVmax (4.19±1.10) and high tissue of interest-to-blood ratios (3.57±0.90) (Fig. 3c). Another patient's lung mass was an inflammatory pseudotumor, which also showed definite RGD uptake with an SUVmax of 9.05 and a high tumour-to-blood ratio of 6.62 in the ^{18}F-alfatide RGD PET imaging (Fig. 3d).

The SUV uptake values and tumour-to-blood ratios of all the tumours are summarized in Table 3.

The SUV for malignant lesions was 5.37±2.17, significantly higher than that for hamartomas (1.60±0.11; $P<0.001$). The difference between the tumour-to-blood ratio for malignant lesions (4.13±0.91) and hamartomas (1.56±0.24) was also statistically significant ($P<0.001$). Neither the SUVmax nor the tumour-to-blood ratio was significantly different between malignant lesions and inflammatory lesions or inflammatory pseudotumour ($P>0.05$).

Table 3 Semiquantitative assessment of RGD uptake in lung lesions

Pathologic diagnosis	Total No.	SUV	Tumor-to-blood ratio
Malignant	17	5.37±2.17	4.13±0.91
Benign	9	3.58±2.52	3.02±1.78
Hamartoma	4	1.60±0.11	1.56±0.24
Chronic inflammation	4	4.19±1.10	3.57±0.90
Inflammatory pseudotumor	1	9.05	6.62

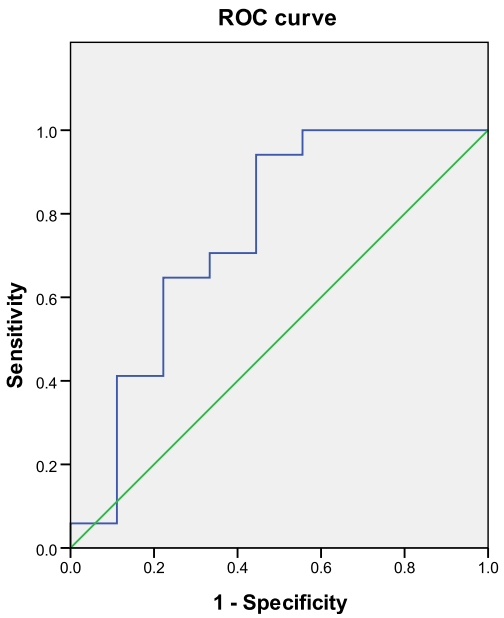

Fig. 4 ROC curves showing diagnostic performance of ^{18}F-RGD PET in suspected lung cancer patients

Table 4 Clinicopathological characteristics and RGD uptake in patients with non-small cell lung cancer

Characteristic	No. of patients	SUVmax (means±SD)	Tumor-to-blood ratio (means±SD)
Total	17	5.37±2.17	4.13±0.91
Pathological subtybe			
Squamous carcinoma	9	5.92±2.97	4.44±0.90
Adenocarcinoma	6	5.37±1.72	4.00±0.99
Adenosquamous carcinoma	2	3.77±0.75	3.80±0.71
P value		0.51	0.60
Differentiation			
Well	3	3.82±1.28	3.85±0.41
Moderate	7	5.73±2.75	3.93±1.16
Poor	7	5.69±1.71	4.46±0.77
P value		0.42	0.50

Using the new scale, ^{18}F-alfatide RGD PET/CT correctly recognized 17 patients with lung cancer, 4 patients as true negative, 5 patients as false positive, and no patients as false negative. Hence, the sensitivity, specificity, accuracy, PPV and NPV of ^{18}F-alfatide RGD PET/CT for the diagnosis of suspected lung cancer patients was 100, 44.44, 80.77, 77.27, and 100 %, respectively. In the ROC curve (Fig. 4), the area under the curve was 0.75 (P=0.038), and ROC analysis suggested a SUVmax cut-off value of 2.65 to differentiate between malignant lesions and benign lesions.

The correlation of clinicopathological characteristics and RGD uptake

The clinicopathological characteristics and the RGD uptake of lesions are summarized in Table 4. No significant correlation was observed between the RGD SUVmax (or tumour–to–blood ratio) and differentiation of cancer cells or pathological subtype.

The mean size of all tumours as determined by histopathologic analysis or CT was 3.24±1.47 cm. The tumour size and SUV were not correlated (P=0.40, R=0.25) (Fig. 5).

Assessment of locoregional lymph nodes

Of the 26 patients, 16 underwent successful surgery. A total of 152 lymph nodes were evaluated by pathologic analysis. Of these, 14 (9 %) lymph nodes were positive for malignancy. The ^{18}F-alfatide RGD PET/CT confirmed 13 metastatic lymph nodes with a mean SUV of 2.23±0.43 (range, 1.64–2.99) and lymph node-to-blood ratios of 3.21 ±0.66 (range, 1.96–4.31) (Fig. 6), 132 lymph nodes as true negative, 6 lymph nodes as false positive, and only 1 lymph node as false negative, resulting in a sensitivity of 92.86 %, specificity of 95.65 %, and accuracy of 95.40 %. The PPV was 61.9 % and the NPV was 99.25 % (Table 5). The negative lymph nodes had a mean SUV of 0.91±0.33 (range, 0.47–1.82) and lymph node-to-blood ratios of 1.39 ±0.36 (range, 0.78–2.06).

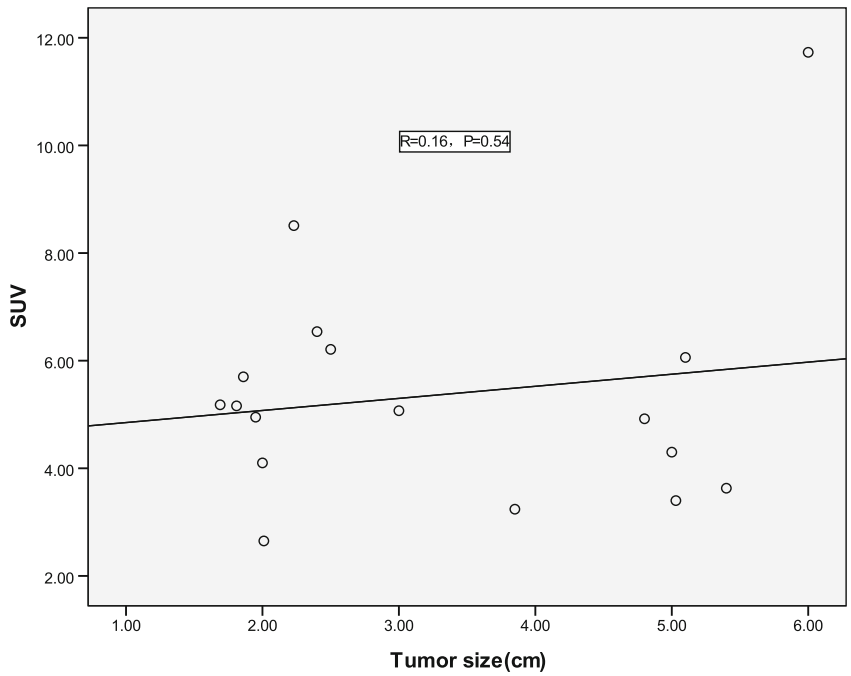

Fig. 5 The correlations between tumor size and tumor SUV

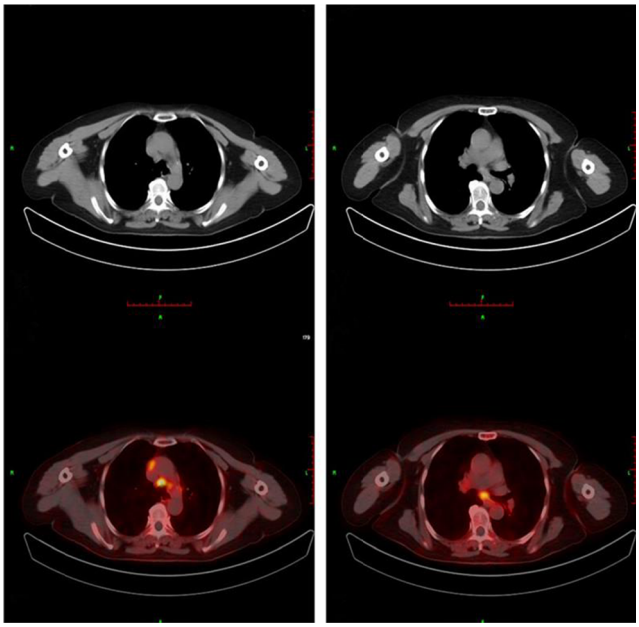

Fig. 6 High uptake in metastasis lymph nodes in lung cancer patient at 1 h after injection of ^{18}F-alfatide are shown

Detection of distant metastatic lesions

In this study, 3 bone metastatic lesions were detected by ^{18}F-alfatide RGD PET/CT, with an SUV of 4.71±0.96 (Fig. 7). No other distant metastases were observed.

Discussion

Our results show that ^{18}F-alfatide RGD PET/CT using the new tracer ^{18}F-alfatide is safe and effective. All tumours could be clearly identified by ^{18}F-alfatide. ^{18}F-alfatide RGD PET/CT may be used for the diagnosis of lung cancer and it can aid in distinguishing hamartoma from malignant lung lesions, as well as to detect distant metastases. It also has important value in the assessment of locoregional lymph nodes for patients with non-small cell lung cancer, but it remains difficult to clearly differentiate inflammatory or inflammatory pseudotumours from malignant lesions.

Many studies have demonstrated that RGD PET/CT can identify several tumour types, such as breast cancer [23, 26], malignant glioma [27], and squamous cell carcinoma of the head and neck [28]. In those studies, the complex synthesis of other RGD peptides hampered its broad use in large clinical studies. In this research, we applied a new tracer, ^{18}F-alfatide, using an improved and simpler labelling method, which makes it possible to use clinically. It yields satisfactory image contrast and clear identification of tumours and metastatic lesions, as well as other information.

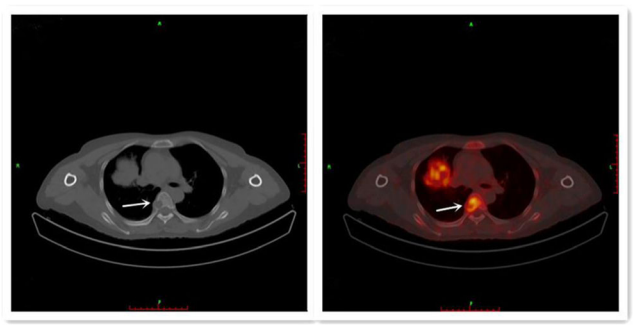

Fig. 7 Transaxial PET/CT image covering bone metastatic lesion, 1 h after injection of ^{18}F-alfatide. Arrows point to the bone metastatic lesion

Angiogenesis is one of the early pathological changes of chronic inflammation, and the inflammatory process is often accompanied by angiogenesis and the formation of new blood vessels. Thus, chronic inflammation and inflammatory pseudotumours showed high uptake in the ^{18}F-alfatide RGD PET, and the five patients were diagnosed as false positive. These results lead to the low specificity.

On the other hand, ^{18}F-alfatide RGD PET was useful for diagnosing nodal involvement. The sensitivity, specificity, and accuracy are similar to previous studies of FDG PET [32–34]. In this study, all false-positive lymph nodes were from the patient with benign chronic inflammatory disease and were attributed to the inflammatory process often accompanying angiogenesis. We only found one false-negative lymph node, an interlobar lymph node, because the diameter was too small and was not identified by CT.

Our results demonstrated the tumour size and SUV were not correlated, which we thought may be related to its imaging principle, ^{18}F-alfatide RGD PET/CT targeting $\alpha v\beta 3$ for imaging tumour angiogenesis, but angiogenesis did not depend on tumor size; a small tumor may have more new blood vessels. Thus, ^{18}F-alfatide RGD uptake occurred in all primary tumor lesions, which was very heterogeneous and did not depend on tumor size. Tracer uptake in metastases also was very heterogeneous.

Although this prospective study of RGD PET/CT with ^{18}F-alfatide was performed successfully, it has the following deficiencies: (1) The number of patients was small; larger cohorts are required to confirm these findings. An additional study is required to recruit a broad variety of patients with lung lesions

Table 5 The sensitivity, specificity, accuracy, PPV, and NPV of PET/CT scans for lymph node

Parameter	TP	TN	FP	FN	Sensitivity	Specificity	Accuracy	NPV	PPV
RGD PET/CT	13	132	6	1	92.86 %	95.65 %	95.40 %	99.25 %	61.90 %

TP true positive, *FN* false-negative, *FP* false-positive, *TN* true negative, *PPV* positive predictive value, *NPV* negative predictive value

to determine the sensitivity, specificity, and accuracy of ^{18}F-alfatide RGD PET/CT; (2) Because the benign chronic inflammatory lesion had definite RGD uptake, it is still difficult to clearly differentiate it from malignant lesions; and (3) The kidneys, liver, spleen and intestines also showed higher uptake, so ^{18}F-alfatide RGD PET/CT is not suitable for tumours and metastatic lesions of the liver, kidney and intestines.

Unlike FDG PET, ^{18}F-alfatide RGD PET has a poor uptake in the brain, brain ventricles and neck, while tumour uptake is very heterogeneous, resulting in good image contrast. It may be more applicable to tumours of the head and neck. Antiangiogenic therapy is burgeoning and promising in the treatment of some cancers, including lung cancer. Antiangiogenic therapy is mainly to inhibit the tumor growth and transfer instead of directly killing them, so it is unable to cause the tumors to shrink rapidly in the short-term and is difficult to evaluate by CT or FDG PET/CT. Based on different imaging principles, ^{18}F-alfatide RGD PET/CT, as a promising angiogenesis imaging tool, may play a more important role than glucose metabolic imaging, FDG PET/CT, in the evaluation of lung cancer**.** In future research, it is necessary to explore the therapeutic evaluation ability of this imaging method in anti-angiogenesis applications.

Conclusion

Our results suggest that RGD PET/CT with the new tracer ^{18}F-alfatide is safe and potentially effective in the diagnosis of non-small cell lung cancer. Further studies with a larger number of patients are needed to validate our findings.

Compliance with Ethical Standards

Funding This study was funded by the Natural Science Foundation of China (NSFC81172133, NSFC81372413), the special fund for Scientific Research in the Public Interest (201402011), the projects of medical and health technology development program in Shandong province (2014WS0058) and the Outstanding Youth Natural Science Foundation of Shandong Province (JQ201423). No other potential conflicts of interest relevant to this article are reported.

Conflict of interest The authors declare that there are no conflicts of interests.

Ethical standards Our investigation of 26 patients was approved by the Shandong Cancer Hospital & Institute Ethical Committee and has, therefore, been performed in accordance with the ethical standards laid down in the 1964 Declaration of Helsinki. All persons gave their informed consent prior to their inclusion in the study.

References

1. Jain RK. Normalization of tumor vasculature: an emerging concept in antiangiogenic therapy. Science. 2005;307:58–62.
2. Folkman J. Tumor angiogenesis: therapeutic implications. N Engl J Med. 1971;285:1182–6.
3. Botrel TE, Clark O, Clark L, Paladini L, Faleiros E, Pegoretti B. Efficacy of bevacizumab (Bev) plus chemotherapy (CT) compared to CT alone in previously untreated locally advanced or metastatic non-small cell lung cancer (NSCLC): systematic review and meta-analysis. Lung Cancer. 2011;74:89–97.
4. Niu G, Chen X. Why integrin as a primary target for imaging and therapy. Theranostics. 2011;1:30–47.
5. Liu S. Radiolabeled cyclic RGD peptides as integrin alpha(v)beta(3)-targeted radiotracers: maximizing binding affinity via bivalency. Bioconjug Chem. 2009;20:2199–213.
6. Danhier F, Le BA, Preat V. RGD-based strategies to target alpha(v) beta(3) integrin in cancer therapy and diagnosis. Mol Pharm. 2012;9:2961–73.
7. Beer AJ, Kessler H, Wester HJ, Schwaiger M. PET imaging of integrin alphaVbeta3 expression. Theranostics. 2011;1:48–57.
8. Battle MR, Goggi JL, Allen L, Barnett J, Morrison MS. Monitoring tumor response to antiangiogenic sunitinib therapy with 18F-fluciclatide, an 18F-labeled alphaVbeta3-integrin and alphaV beta5-integrin imaging agent. J Nucl Med. 2011;52:424–30.
9. Ruoslahti E, Pierschbacher MD. New perspectives in cell adhesion: RGD and integrins. Science. 1987;238:491–7.
10. Haubner R, Wester HJ, Reuning U, Senekowitsch-Schmidtke R, Diefenbach B, Kessler H, et al. Radiolabeled alpha(v)beta3 integrin antagonists: a new class of tracers for tumor targeting. J Nucl Med. 1999;40:1061–71.
11. Beer AJ, Schwaiger M. PET imaging of alphavbeta3 expression in cancer patients. Methods Mol Biol. 2011;680:183–200.
12. Chen X, Park R, Shahinian AH, Tohme M, Khankaldyyan V, Bozorgzadeh MH, et al. 18F-labeled RGD peptide: initial evaluation for imaging brain tumor angiogenesis. Nucl Med Biol. 2004;31:179–89.
13. Jeong JM, Hong MK, Chang YS, Lee YS, Kim YJ, Cheon GJ, et al. Preparation of a promising angiogenesis PET imaging agent: 68Ga-labeled c(RGDyK)-isothiocyanatobenzyl-1,4,7-triazacyclononane-1,4,7-triacetic acid and feasibility studies in mice. J Nucl Med. 2008;49:830–6.
14. Li ZB, Chen K, Chen X. (68)Ga-labeled multimeric RGD peptides for microPET imaging of integrin alpha(v)beta (3) expression. Eur J Nucl Med Mol Imaging. 2008;35:1100–8.
15. Chen X, Liu S, Hou Y, Tohme M, Park R, Bading JR, et al. MicroPET imaging of breast cancer alphav-integrin expression with 64Cu-labeled dimeric RGD peptides. Mol Imaging Biol. 2004;6:350–9.
16. Lang L, Li W, Jia HM, Fang DC, Zhang S, Sun X, et al. New methods for labeling RGD peptides with bromine-76. Theranostics. 2011;1:341–53.
17. Jacobson O, Zhu L, Niu G, Weiss ID, Szajek LP, Ma Y, et al. MicroPET imaging of integrin alphavbeta3 expressing tumors using 89Zr-RGD peptides. Mol Imaging Biol. 2011;13:1224–33.
18. Haubner R, Weber WA, Beer AJ, Vabuliene E, Reim D, Sarbia M, et al. Noninvasive visualization of the activated alphavbeta3 integrin in cancer patients by positron emission tomography and [18F]Galacto-RGD. PLoS Med. 2005;2:e70.
19. Haubner R, Wester HJ, Weber WA, Mang C, Ziegler SI, Goodman SL, et al. Noninvasive imaging of alpha(v)beta3 integrin expression using 18F-labeled RGD-containing glycopeptide and positron emission tomography. Cancer Res. 2001;61:1781–5.
20. Beer AJ, Haubner R, Goebel M, Luderschmidt S, Spilker ME, Wester HJ, et al. Biodistribution and pharmacokinetics of the

alphavbeta3-selective tracer 18F-galacto-RGD in cancer patients. J Nucl Med. 2005;46:1333–41.
21. Beer AJ, Haubner R, Sarbia M, Goebel M, Luderschmidt S, Grosu AL, et al. Positron emission tomography using [18F]Galacto-RGD identifies the level of integrin alpha(v)beta3 expression in man. Clin Cancer Res. 2006;12:3942–9.
22. McParland BJ, Miller MP, Spinks TJ, Kenny LM, Osman S, Khela MK, et al. The biodistribution and radiation dosimetry of the Arg-Gly-Asp peptide 18F-AH111585 in healthy volunteers. J Nucl Med. 2008;49:1664–7.
23. Kenny LM, Coombes RC, Oulie I, Contractor KB, Miller M, Spinks TJ, et al. Phase I trial of the positron-emitting Arg-Gly-Asp (RGD) peptide radioligand 18F-AH111585 in breast cancer patients. J Nucl Med. 2008;49:879–86.
24. Doss M, Kolb HC, Zhang JJ, Belanger MJ, Stubbs JB, Stabin MG, et al. Biodistribution and radiation dosimetry of the integrin marker 18F-RGD-K5 determined from whole-body PET/CT in monkeys and humans. J Nucl Med. 2012;53:787–95.
25. Mittra ES, Goris ML, Iagaru AH, Kardan A, Burton L, Berganos R, et al. Pilot pharmacokinetic and dosimetric studies of (18)F-FPPRGD2: a PET radiopharmaceutical agent for imaging alpha(v)beta(3) integrin levels. Radiology. 2011;260:182–91.
26. Beer AJ, Niemeyer M, Carlsen J, Sarbia M, Nahrig J, Watzlowik P, et al. Patterns of alphavbeta3 expression in primary and metastatic human breast cancer as shown by 18F-Galacto-RGD PET. J Nucl Med. 2008;49:255–9.
27. Schnell O, Krebs B, Carlsen J, Miederer I, Goetz C, Goldbrunner RH, et al. Imaging of integrin alpha(v)beta(3) expression in patients with malignant glioma by [18F] Galacto-RGD positron emission tomography. Neuro Oncol. 2009;11:861–70.
28. Beer AJ, Grosu AL, Carlsen J, Kolk A, Sarbia M, Stangier I, et al. [18F]galacto-RGD positron emission tomography for imaging of alphavbeta3 expression on the neovasculature in patients with squamous cell carcinoma of the head and neck. Clin Cancer Res. 2007;13:6610–6.
29. McBride WJ, D'Souza CA, Sharkey RM, Goldenberg DM. The radiolabeling of proteins by the [18F]AlF method. Appl Radiat Isot. 2012;70:200–4.
30. Lang L, Li W, Guo N, Ma Y, Zhu L, Kiesewetter DO, et al. Comparison study of [18F]FAl-NOTA-PRGD2, [18F]FPPRGD2, and [68Ga]Ga-NOTA-PRGD2 for PET imaging of U87MG tumors in mice. Bioconjug Chem. 2011;22:2415–22.
31. Wan W, Guo N, Pan D, Yu C, Weng Y, Luo S, et al. First experience of 18F-alfatide in lung cancer patients using a new lyophilized kit for rapid radiofluorination. J Nucl Med. 2013;54:691–8.
32. Shim SS, Lee KS, Kim BT, Chung MJ, Lee EJ, Han J, et al. Non-small cell lung cancer: prospective comparison of integrated FDG PET/CT and CT alone for preoperative staging. Radiology. 2005;236:1011–9.
33. Yang W, Fu Z, Yu J, Yuan S, Zhang B, Li D, et al. Value of PET/CT versus enhanced CT for locoregional lymph nodes in non-small cell lung cancer. Lung Cancer. 2008;61:35–43.
34. Yuan S, Yu Y, Chao KS, Fu Z, Yin Y, Liu T, et al. Additional value of PET/CT over PET in assessment of locoregional lymph nodes in thoracic esophageal squamous cell cancer. J Nucl Med. 2006;47:1255–9.